Supplementary figures and Tables

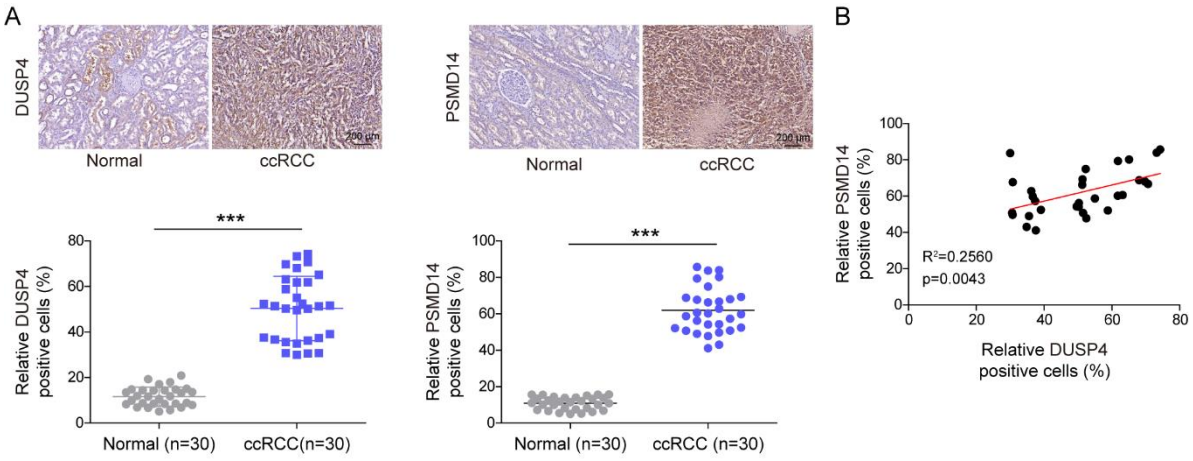

Figure S1. DUSP4 and PSMD14 are co-upregulated and positively correlated in ccRCC tissues. (A) Immunohistochemistry (IHC) was used to detect the expression of DUSP4 and PSMD14 proteins in ccRCC and adjacent noncancerous tissues. (B) Pearson correlation analysis was used to assess the relationship between DUSP4 and PSMD14 protein expression levels in ccRCC samples (n = 30 biologically independent samples).

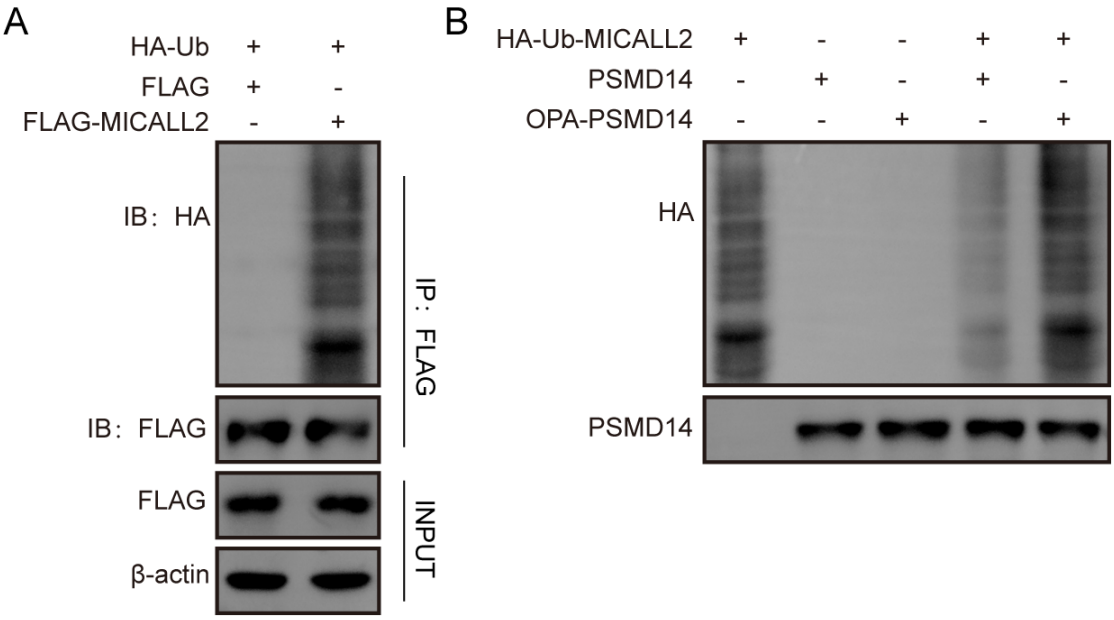

Figure S2. PSMD14 directly deubiquitinates MICALL2 in vitro. (A) Verification of HA-Ub–MICALL2 complexes by immunoprecipitation (IP). The whole-cell lysates (Input) and anti-FLAG immunoprecipitated (IP: FLAG) of 293T cells co-transfected with FLAG-MICALL2 and HA-Ubiquitin were immunoblotted with the indicated antibodies. n = 3 independent experiments. (B) In vitro deubiquitination assay showing direct removal of ubiquitin from MICALL2 by PSMD14 (n = 3 independent experiments). The immunoprecipitated HA-Ub–MICALL2 complexes was incubated in a cell-free system with buffer alone, active PSMD14, or catalytically inactivated PSMD14 pretreated with O-phenanthroline (OPA-PSMD14). The reaction mixture was immunoblotted to detect ubiquitinated MICALL2 (anti-HA) and total MICALL2 (anti-FLAG).

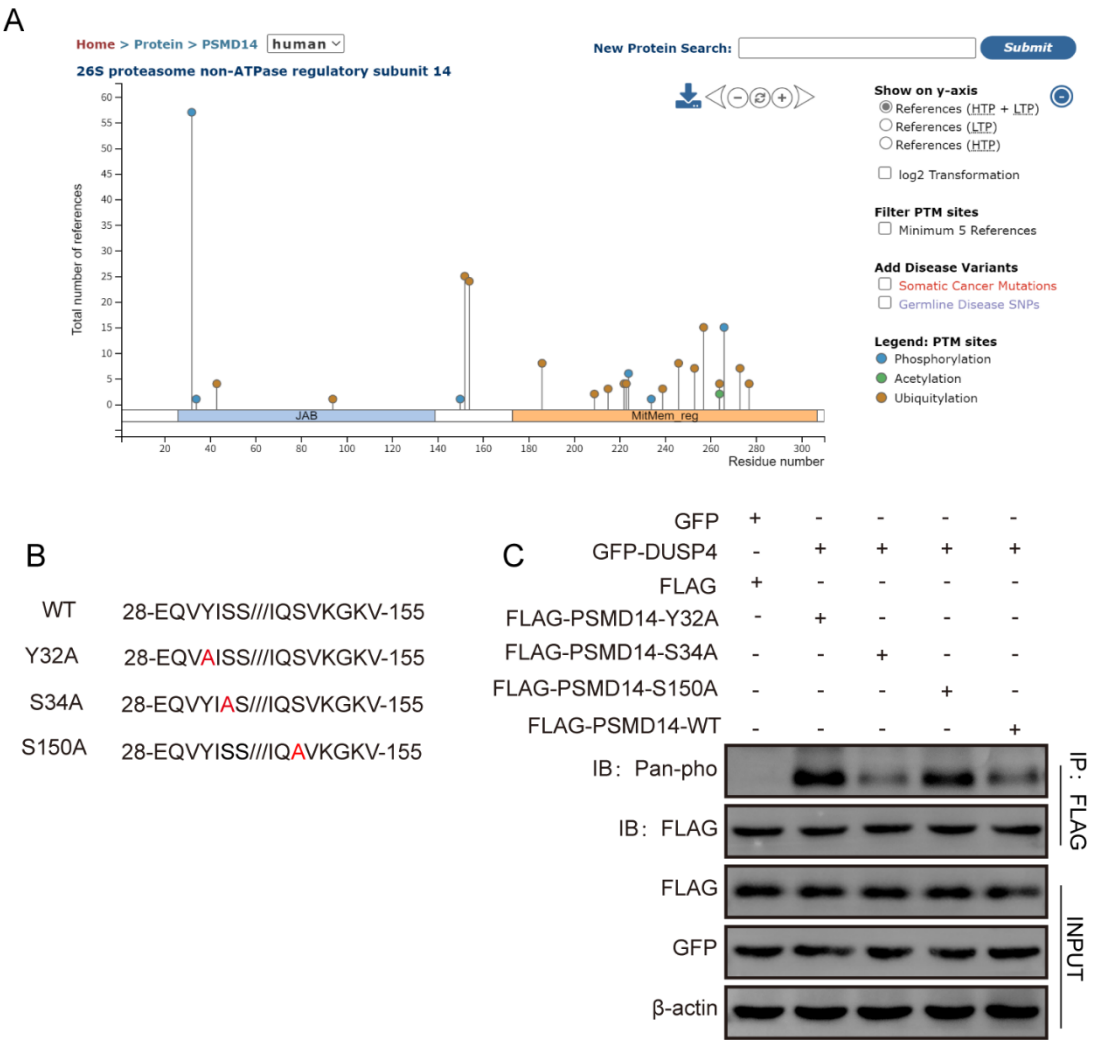

Figure S3. Identification of Y32 and S150 as the critical phosphorylation site on PSMD14 targeted by DUSP4. (A) The PhosphoSitePlus database was used to predict potential phosphorylation sites on PSMD14. (B) Site-directed mutagenesis structure diagram of PSMD14 phosphorylation site mutations (Y32A, S34A, and S150A). (C) Western blot was used to assess the phosphorylation level of PSMD14 in wild-type PSMD14 and site-directed mutant (n = 3 independent experiments), for the purpose of verifying whether residue Y32 and S150 are a critical target site for DUSP4-mediated dephosphorylation. Statistical analysis was performed using one-way ANOVA with Tukey's post-hoc test.

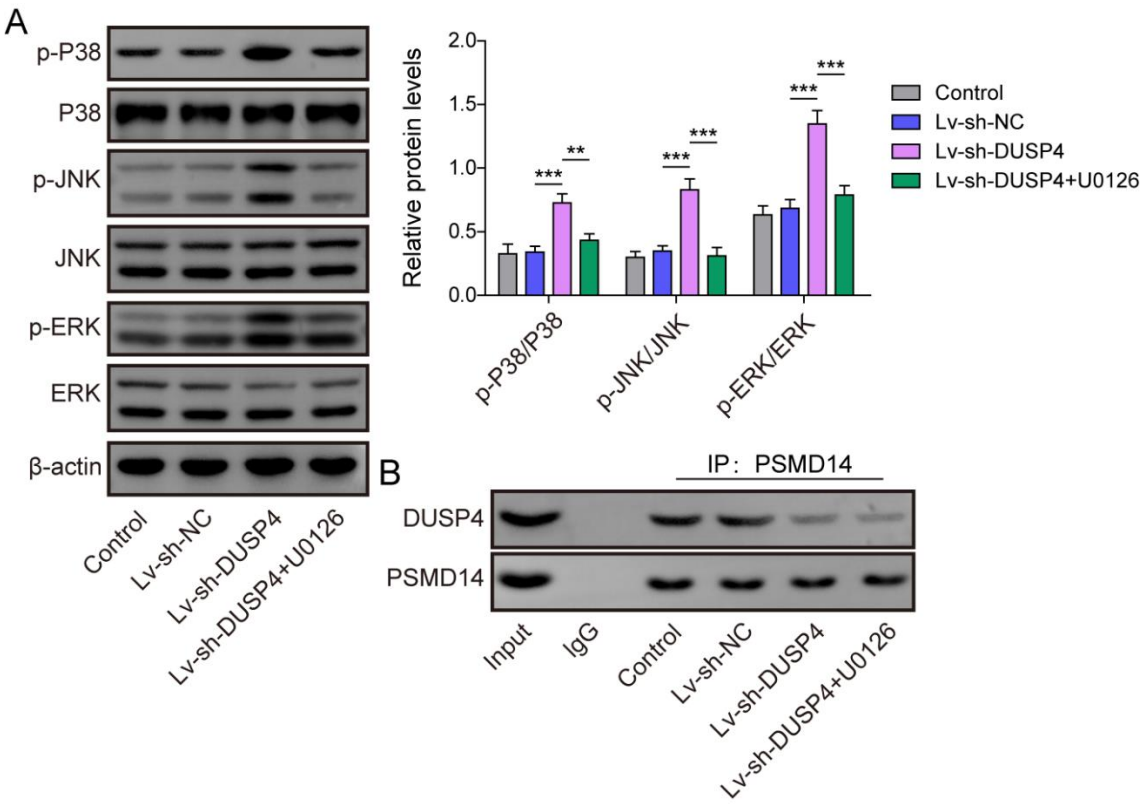

Figure S4. The DUSP4–PSMD14 interaction is independent of MAPK pathway activity. ccRCC cells were subjected to the following treatments: lv-sh-NC, lv-sh-DUSP4, or lv-sh-DUSP4 + MEK inhibitor U0126. n = 3 independent experiments for both panels. (A) Western blot analysis of MAPK pathway components, including the total and phosphorylated forms of p38, JNK, and ERK. (B) Co-immunoprecipitation assay was used to detect the interaction between DUSP4 and PSMD14 under different treatment conditions. One-way ANOVA with Tukey's post-hoc test. $^{**}P < 0.01$, $^{***}P < 0.001$.

Table S1: Correlation between DUSP4 and PSMD14 expression and clinicopathological characteristics of patients with ccRCC

Clinicopathologic features		Cases (n=30)	DUSP4		P-value	Cases (n=30)	PSMD14		P-value
			High (n=15)	Low (n=15)			High (n=15)	Low (n=15)	
Age	＜65	16	7	9	0.7152	16	6	10	0.2723
	≥65	14	8	6		14	9	5	
Gender	Female	13	5	8	0.4621	13	5	8	0.4621
	Male	17	10	7		17	10	7	
Tumor stage	T1-T2	12	1	11	**0.0005**	12	2	10	**0.0078**
	T3-T4	18	14	4		18	13	5	
Tumor size	< 5cm	13	2	11	**0.0025**	13	3	10	**0.0253**
	≥5cm	17	13	4		17	12	5	
Relapse-free survival	Non-relapsed	14	2	12	**0.0007**	14	3	11	**0.0092**
	Relapsed	16	13	3		16	12	4	

Table S2: The primers for knockdown expression and overexpression

Gene Symbol	sequence
MICALL2 overexpression	F primer 5’-GTTCCCAGTTCTCAGCC-3’
	R primer 5’-GATTCCGCCAAGTTCCT-3’
PSMD14 overexpression	F primer 5’-GGAGGAGGTATGCCTGGACT-3’
	R primer 5’-GGTTTTCTCCATGCTGTTTCTT-3’
DUSP4 knockdown (sh-1)	CGGCCTCTACTCGGCGGTCAT
DUSP4 knockdown (sh-2)	CCCAGTGGAAGATAACCACAA
DUSP4 knockdown (sh-3)	GCCTACCTGATGATGAAGAAA
MICALL2 knockdown (sh-1)	CTCAGTTCAAGCTCCACATCT
MICALL2 knockdown (sh-2)	GACGTTTGTGACAACTGGCTT

MICALL2 knockdown (sh-3)	GTTCTGGCTCATTCACGAGAA
PSMD14 knockdown (sh-1)	GTTGGCTTTCTGGTGTGGATA
PSMD14 knockdown (sh-2)	CAAGCCATCTATCCAGGCATT
PSMD14 knockdown (sh-3)	CAGTGAACATTGTAAACACAA
sh-NC	TTCTCCGAACGTGTCACGT